Proceedings of the 2007 IEEE/RSJ International
Conference on Intelligent Robots and Systems
San Diego, CA, USA, Oct 29 - Nov 2, 2007

Experience-based and Tactile-driven Dynamic Grasp Control

Jan Steffen, Robert Haschke and Helge Ritter
Neuroinformatics Group, Faculty of Technology, University of Bielefeld, Germany
{jsteffen,rhaschke,helge}@techfak.uni-bielefeld.de

Abstract— **Algorithms for dextrous robot grasping always have to cope with the challenge of achieving high object specialisation for a wide range of grasping contexts. In this paper, we present a tactile-driven approach that dynamically uses the robot's grasping experience to address this issue. During the grasp movement, the current contact information is used to dynamically adapt the grasping control by targeting the best matching posture from the experience base. Thus, the robot *recalls* and actuates a grasp it already successfully performed in a similar tactile context. To efficiently represent the experience, we introduce the *Grasp Manifold* assuming that grasp postures form a smooth manifold in hand posture space. We present a simple way of providing approximations of *Grasp Manifolds* using Self-Organising Maps (SOMs). The algorithm is evaluated on three different geometry primitives – box, cylinder and sphere – in a physics-based computer simulation.**

I. Introduction

Dextrous robot grasping is a complex task and poses some very intricate problems. One of the main difficulties is to find grasping strategies and algorithms which generalise to new situations and thus are sufficiently robust against variations of object position, orientation, or even shape.

In general, there are two apposing basic approaches to address this issue. The first uses object geometry information to plan the grasp beforehand by computing a geometry-specific (optimal) hand posture. The second closes the fingers around the object solely based on tactile feedback until stable object contact is detected. In the case of "geometry-based" grasping, the algorithm itself inheres the knowledge of how to grasp specific object models, but is not able to explore the presented geometry in order to parametrise the grasp control. On the other side, "contact-based" grasping reacts on tactile events and adapts the grasping motion to the actual situation, but is not able to take advantage of any grasping experience or object knowledge.

For both strategies, several examples exist. Borst et al. [1] compute a set of optimised contact points based on a detailed geometric object model and calculate a hand posture that generates the recommended contacts solving a constrained optimisation problem. Later, they relax the need of optimal contact points showing that an average quality grasp performs sufficiently well in most tasks [2]. Miller et al. [9] weaken the requirement of a precise geometry information using shape primitives which roughly approximate the object's geometry. Based on these primitives, multiple grasp starting positions and approach vectors are evaluated in simulation using GraspIt! [8], and the best one is chosen for execution. Pelossof et al. [11] combine this approach with SVM regression to map parametric descriptions of superquadric objects to potential initial hand postures and an associated grasp quality. In real world scenarios grasping every-day objects, this kind of approach has the drawback that (even a coarse) geometrical object model is usually not available. Thus, the precise grasping knowledge cannot be optimally exploited due to the lack of object knowledge.

The contact-based grasping uses no object information and is thus better qualified in unknown grasping situations. Such a control has been presented by Natale and Torres-Jara [10] who built a tactile-driven system to explore and grasp objects without prior object knowledge. They conclude that tactile exploration is more powerful in every-day tasks than precise a priori computation. Platt et al. [12], [13] treat grasping as an active sensory-driven problem without explicit object knowledge. Multiple control laws are applied whereas subordinate laws operate in the nullspace of superordinate ones and hence do not interfere with higher level goals. In previous works, we proposed an algorithm based on pairs of an initial pre-grasp and a final grasp posture which are selected from a set of common grasps according to human gestures [18], [16]. The grasp is accomplished by a tactile-driven transition from the initial pre-grasp to the final grasp posture, stopping when stable fingertip contacts are detected. Solely based on tactile feedback and without any assumptions on the object shape, all purely contact-based approaches cannot exploit object-specific knowledge to perform expedient task-dependent finger coordination.

In the present paper, we propose a new approach to dextrous robot grasping that combines the advantages of geometry-based and contact-based grasping. Using tactile information to infer implicit object knowledge, the algorithm dynamically includes previously acquired grasping knowledge to adapt the grasping motion to the actual situation. The grasping experience is formed by a database of hand postures which previously led to successful grasps. According to observed finger contacts, the most suitable hand posture is selected from the database to guide the grasping process. To improve computational performance and generalisation we propose a compact representation of the database as a low-dimensional manifold in the space of all possible hand postures. More concretely, we employ object-specific Self-Organising Maps (SOMs) to approximate this manifold by a few number of discrete postures.

The implementation, acquisition of training data, and evaluation have been realised in a physics-based computer simulation using the proprietary toolkit VORTEX [3] and

1-4244-0912-8/07/$25.00 ©2007 IEEE.

a model of our 24-DOF SHADOW DEXTROUS HAND [19] shown in Fig. 1. While the kinematics of the hand model exactly corresponds to the real hand, the geometric shape is only coarsely approximated which has proven to be sufficient to obtain results applicable to the real hand.

The paper is organised as follows: In Section II the proposed grasping algorithm is presented in detail assuming an arbitrary representation of the experience database. In Section III we recall the SOM algorithm and discuss advantages and disadvantages of this compact representation. The evaluation of the algorithm for three basic object shapes is described in Section IV and finally we discuss the results in Section V.

II. EXPERIENCE-BASED GRASPING

The main idea of the proposed grasping algorithm is to augment a tactile-driven grasping heuristics with an *experience base of grasp postures* which can be used to guide the grasping process to promising hand postures. We represent this experience as a database of hand postures $\vec{\Theta}$ which previously led to successful grasps of one or more objects in a variety of grasping contexts, i.e. different positions and orientations of the object relative to the hand. Let I be the number of fingers, N_i the most distal joint in finger i, then $\vec{\Theta}$ denotes the vector $[\Theta_{1,1},\ldots,\Theta_{1,N_1},\Theta_{2,1},\ldots,\Theta_{I,N_I}]^t$ comprising all finger joint angles. Notice, that a grasp posture directly corresponds to a specific object and grasping context. Used in another context, the same hand posture might not lead to a successful grasp.

Comprising a set of successful grasp postures, the experience base implicitly provides knowledge of how to grasp the associated object. As counterpart, the tactile information observed during the grasping process provides implicit knowledge of the actual object shape, position and orientation. A dynamic matching of this context-specific knowledge to the grasping knowledge stored in the experience base yields information about how to grasp the current object in the current situation. We only utilise joint angles for this matching process whose finger segments provide reliable context information. To this end, we employ a *Partial Contact Posture (PCP)* $\vec{\Theta}^{pcp}$ specifying only joints between the palm and finger segments having object contact. If $S_{i,j}$ denotes the finger segment directly attached to and moved by joint j of finger i, the PCP can be defined more formally as:

$$\vec{\Theta}^{pcp} = [\Theta^{pcp}_{1,1},\ldots,\Theta^{pcp}_{1,N_1},\Theta^{pcp}_{2,1},\ldots,\Theta^{pcp}_{I,N_I}]^t \quad \text{where:}$$

$$\Theta^{pcp}_{i,j} = \begin{cases} \Theta_{i,j} & \text{if a segment } S_{i,(k\geq j)} \text{ has contacts} \\ \text{not specified} & \text{otherwise.} \end{cases}$$

Based on this PCP, we define a modified Euclidean norm d^{pcp} to match a current hand posture $\vec{\Theta}^{pcp}$ to the best matching posture $\vec{\Theta}^{xp,\star}$ in the experience base $\{\vec{\Theta}^{xp}\}$ by minimising d^{pcp}, only taking reliable joints into account:

$$d^{pcp}(\vec{\Theta}^{xp},\vec{\Theta}^{pcp}) = \sum_{i,j} s_{i,j}\cdot(\Theta^{xp}_{i,j}-\Theta^{pcp}_{i,j})^2 \qquad (1)$$

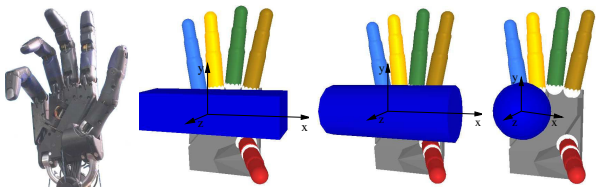

Fig. 1. The Shadow Dextrous Hand and its virtual simulation model. Depicted is the initial hand posture with the three studied grasp objects: 1) box (4×4×16cm), 2) cylinder (l:16cm, ∅:6cm), and 3) sphere (∅:6cm).

The $s_{i,j}\in\{0,1\}$ only select *specified dimensions* of $\vec{\Theta}^{pcp}$ for comparison. As the PCP requires contact information, a precondition for the experience-based control is the existence of at least one contact. Furthermore, as the experience base is a discrete set of hand postures which additionally is affected by noise, a subsequent generic finger closing heuristic similar to our originally used algorithm [16] is necessary to establish stable object contacts.

Subsumed, there are four different control phases of the algorithm: A) Actuating an initial hand posture, B) Establishing first contact in an already experience-influenced process, C) Performing experience-based grasp control and D) Applying a generic finger closing heuristic (embedded in phases B and C). The whole grasp control is embedded in an action-perception-loop which allows a dynamic adaptation to the current grasping context. A schematic overview of the control algorithm is given in Fig. 2. Single loop iterations will be referred to as *control cycles*.

A. Initial hand posture (Pregrasp) (Fig. 2A)

While our previous, purely contact-based grasping algorithm is based on a static transition from an initial to a final hand posture [16], the experience-based approach dynamically selects the currently best fitting hand postures from the experience base to finally reach a grasp posture optimally suited for the actual situation. Nevertheless, the grasping result depends on the initial hand posture which actually pre-determines the first contact occurrence and thus primes the remaining grasping process. Hence, the *pre-grasp* posture should be selected context-dependent, e.g. incorporating task knowledge or vision results. From experiments, we know that the new algorithm is relatively robust with respect to the initial hand posture and we used the posture shown in Fig. 1(right) for all evaluation experiments.

B. Establishment of first contact (Fig. 2B)

Prior to the first contact, the best-match search based on Eq.1 cannot be applied because no meaningful PCP is available. Nevertheless, the experience base contains valuable information about typical grasp postures. Hence, within this initial phase we actuate the posture $\vec{\Theta}^{xp,\star}$ which best resembles the current posture considering *all* joint angles ($\vec{\Theta}^{pcp}=\vec{\Theta},\forall i,j: s_{i,j}=1$, cp. Eq. 1). If no contact can be evoked in this manner, the generic finger closing heuristic closes the fingers further until another best-match posture $\vec{\Theta}^{xp,\star}$ is found and the process can start over. This cycle is repeated until the first contact arises.

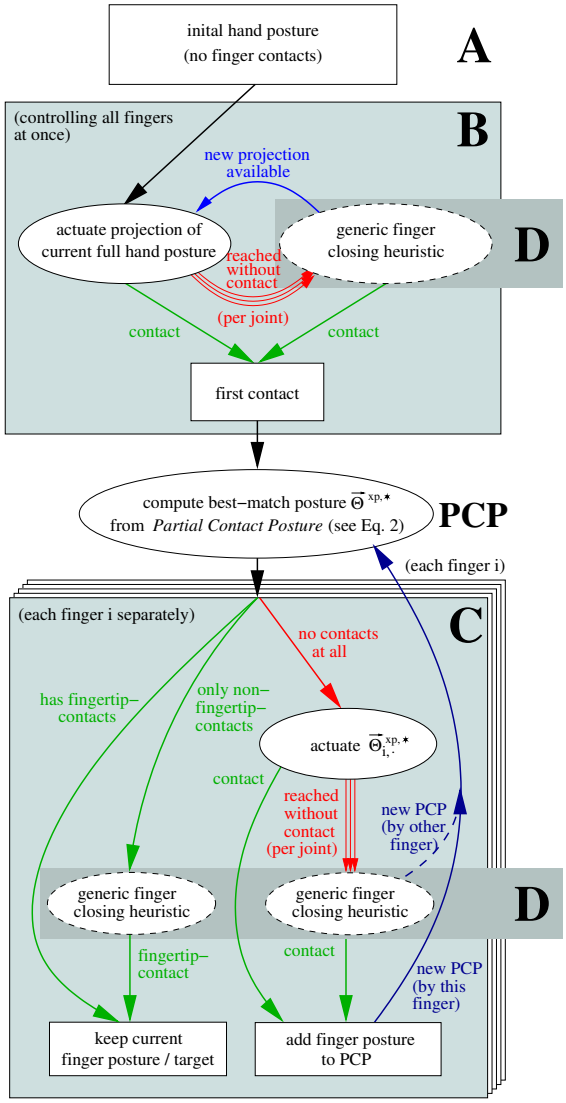

Fig. 2. Overview of the grasp control algorithm.

C. Experience-based control (Fig. 2C)

Initiated by the first contact, the experience-based grasp control considers the current tactile information to determine the best matching posture $\vec{\Theta}^{xp,\star}$ from the experience base:

$$\vec{\Theta}^{xp,\star}(\vec{\Theta}^{pcp}) = \arg\min_{\vec{\Theta}^{xp}} d^{pcp}(\vec{\Theta}^{xp}, \vec{\Theta}^{pcp}) \qquad (2)$$

which is used as target posture for further motion generation. To obtain a stable grasp which additionally allows flexible manipulation of the grasped object, we aim at stable fingertip contacts for all fingers. On the one hand, this ensures that all DOFs can be exploited for manipulation and on the other hand guarantees the highest spatial resolution for tactile sensing. According to Fig. 2C, each finger is controlled separately depending on its particular contact state:

1) The finger has no contact(s).
In this case the finger joints are actuated towards the sub target posture $\vec{\Theta}^{xp,\star}_{i,\cdot}$ corresponding to this finger. If the resulting motion leads to a contact, the PCP changes, a new best-match posture can be computed, and control proceeds in state 2) or 3). If the targeted joint angles are reached without evoking any contacts, the generic finger closing heuristic is applied to further close the finger joints.

2) The finger has only non-fingertip contact(s).
As the former grasp motion did not lead to fingertip contacts, all joints more distal than the contact segment(s) will be subsequently closed further applying the generic finger closing heuristic again. More proximal joints (corresponding to the specified dimensions of the PCP) maintain their current positions to prevent pushing the object away. In this state, the finger control is no longer affected by updates of $\vec{\Theta}^{xp,\star}$ as long as at least one finger contact remains. This prevents backward movements potentially resulting from new target postures and thus ensures a coherent grasping advance.

3) The finger has fingertip contact(s)
The grasping objective is accomplished with respect to this finger and motion of this finger is halted until the fingertip contact is lost, e.g. due to object motion. In that case, the finger control returns to state 1) or 2) in the next cycle.

If the contact situation changes due to finger motions, the PCP is newly determined and a new best-match posture is selected from the experience database as indicated by the bottom-up arrow in Fig. 2C. Hence during grasping progress, the targeted grasp posture is always dynamically adapted to the actual context inferred implicitly from tactile data.

D. Generic finger closing heuristic (Fig. 2D)

If the grasping experience does not cover the current grasping situation, the described control scheme possibly leads to no fingertip contacts at all – even if the targeted posture $\vec{\Theta^{xp,\star}}$ is reached. For example, if the current object is smaller than all previously grasped objects or is shifted in an unusual way. In this case, we apply a modification of our original closing heuristic (cf. [16]) without taking the experience base into account. The aim is to continue the finger closing motion until contacts are observed. The main issue to be handled in this phase is the degree of finger flexion determined by the relative closing speeds of the proximal with respect to the distal finger joints, denoted by the ratio λ. A value $\lambda > 1$ corresponds to a marginal, a value $\lambda \approx 1$ to a distinct flexion. Throughout this paper, we use the empirically determined value $\lambda = 5$, an adaptation of λ according to e.g. vision results is possible but beyond the scope of this paper. The finger joints continue closing at joint-specific speeds $\dot{\Theta}_{i,j}$ according to the following equations:

$$\dot{\Theta}_{i,j} = \begin{cases} 0 & \text{if a segment } S_{i,(k\geq j)} \text{ has contacts} \\ \gamma_{i,j} & \text{otherwise} \end{cases} \qquad (3)$$

$$\text{where} \quad \gamma_{i,j} = \begin{cases} \lambda \cdot \gamma & \text{if } (i,j)\text{: proximal joint} \\ \gamma & \text{otherwise} \end{cases} \qquad (4)$$

The value γ specifies the motion speed which is assumed to be positive to generate a closing motion. Assuming an adequate experience base with appropriate grasp postures, the

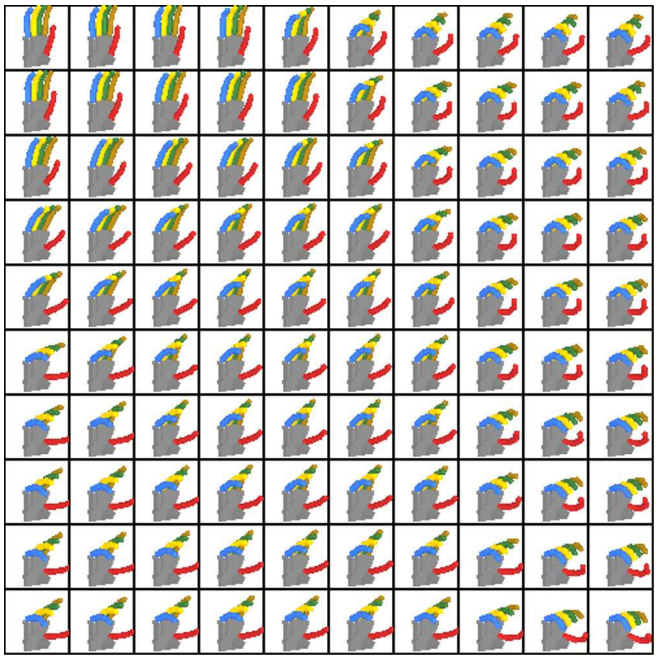

Fig. 3. A two-dimensional 10x10 SOM-based *discrete Grasp Manifold* trained with 4220 cylinder grasp postures over 150 epochs. Each grasp picture represents the reference vector of a single node.

generic finger closing heuristic is only applied to compensate for small deviations of the current grasping situation. In the opposite case, having a poorly matching experience base, the grasp motion is mainly controlled by the purely tactile-driven heuristic. If the grasp succeeds, it can be added to the experience base to improve future grasping.

III. The Grasp Manifold

Grasping experience was introduced in the previous sections as a set of grasp postures. To appropriately cover all possible grasping situations, the database must comprise a multitude of corresponding postures, which increases both the computational costs and required storage capacity. To obtain a more compact representation of the grasping knowledge, we assume that all valid grasp postures for at least one object form a low-dimensional smooth manifold $\mathcal{GM}$ embedded in hand posture space and denote it as *Grasp Manifold*. We further assume that – based on a discrete training set – we can find a discrete approximation $\mathcal{GM}_{dc}$ to $\mathcal{GM}$.

One powerful and adaptive realisation of such an approximation is the Self-Organising Map (SOM), [15]. In terms of the *Grasp Manifold*, it consists of a m-dimensional lattice A of nodes labelled with a spatial lattice index $\vec{a} \in A$ and having attached a reference vector $\vec{w}_{\vec{a}}$ in hand posture space. A projection of a hand posture $\vec{\Theta}$ onto the SOM is determined as the reference vector of the "best-match node"

$$\vec{w}_{\vec{a}^\star}(\vec{\Theta}) = \arg\min_{\vec{w}_{\vec{a}}} \parallel \vec{w}_{\vec{a}} - \vec{\Theta} \parallel . \quad (5)$$

Adaptation of the nodes is realised in an iterative procedure similar to vector quantisation methods. Given a training set $\{\vec{\Theta}_i\}$ of grasp postures the learning rule takes the form:

$$\forall \vec{\Theta}_i : \forall \vec{a}_j : \Delta \vec{w}_{\vec{a}_j}(t) = \varepsilon(t) \cdot h_{\vec{a}_j, \vec{a}^\star(\vec{\Theta}_i)} \cdot (\vec{\Theta}_i - \vec{w}_{\vec{a}_j}) \quad (6)$$

where $t = 1..T$ is the training epoch (cycle over all data points), $\varepsilon(t) \in [0, 1]$ is a slowly decreasing learning rate and $h_{\vec{a}_j, \vec{a}^\star(\vec{\Theta}_i)}$ is a gaussian neighbourhood function diminishing the learning rate depending on the distance of node $\vec{a}_j$ to the best-match node $\vec{a}^\star(\vec{\Theta}_i)$ in the lattice A:

$$h_{\vec{a}, \vec{a}^\star} = \exp\left(-\frac{\parallel \vec{a} - \vec{a}^\star \parallel^2}{2\sigma(t)^2}\right). \quad (7)$$

Due to this neighbourhood adaptation, the SOM can learn a smooth *Grasp Manifold* which preserves the topology of the original hand posture space. The best-match search performed by Eq. 2 within the whole posture base is now replaced by a projection onto the *Grasp Manifold* $\mathcal{GM}_{dc}$ by applying Eq. 5. Projections of a PCP can be realised by adjusting the Euclidean distance computation in Eq. 5 according to Eq. 1.

In the presented work, we use object-specific 25x25 SOMs trained on grasp postures for one specific object shape. Hence, a particular SOM is only adequate to grasp objects of the matching type, requiring a prior classification of the object. This has the advantage, that the extension of the system by new objects does not change the behaviour for already learned objects. Nevertheless, we have shown that representing all grasp postures corresponding to various object shapes *within a single SOM* is possible as well [17]. Fig. 3 depicts a two-dimensional SOM-based *Grasp Manifold* trained on 4220 cylinder grasp postures. Each hand picture represents the reference vector $\vec{w}_{\vec{a}}$ of a particular SOM node. The visualisation of the SOM shows that similar hand postures are grouped together which supports our initial assumption of a smooth low-dimensional *Grasp Manifold*.

IV. Evaluation

The evaluation of the grasp strategy including the execution of the grasps and the evaluation of their stability has been performed in a physics-based 3D computer simulation using the proprietary toolkit VORTEX [3] and the graphical simulation toolkit NEO/NST [14]. As grasp stability measure we use the magnitude α of the worst-case disturbance wrench within the L1 grasp wrench space [4]. In particular, a value $\alpha > 0$ characterises a force closure grasp. The evaluation set-up consists of the *ShadowHand*-model and the object which is hovering in front of the hand due to zero-gravity conditions (cf. Fig. 1). While the palm is fixated in the world, the object can move freely.

To train the object-specific SOM-*Grasp Manifolds*, a set of 10.174 grasp postures was generated in simulation for all three evaluated objects: box (4069 postures), cylinder (4220 post.) and sphere (1885 post.). Training data was presented within all 300 learning epochs according to a random distribution ($\varepsilon(t)$ decreasing from 0.95 to 0.05, $\sigma(t)$ decreasing from 6 to 0.7, cp. Eq. 6 - 7).

To verify the generalisation ability of the discrete *Grasp Manifolds* with respect to position and orientation of the

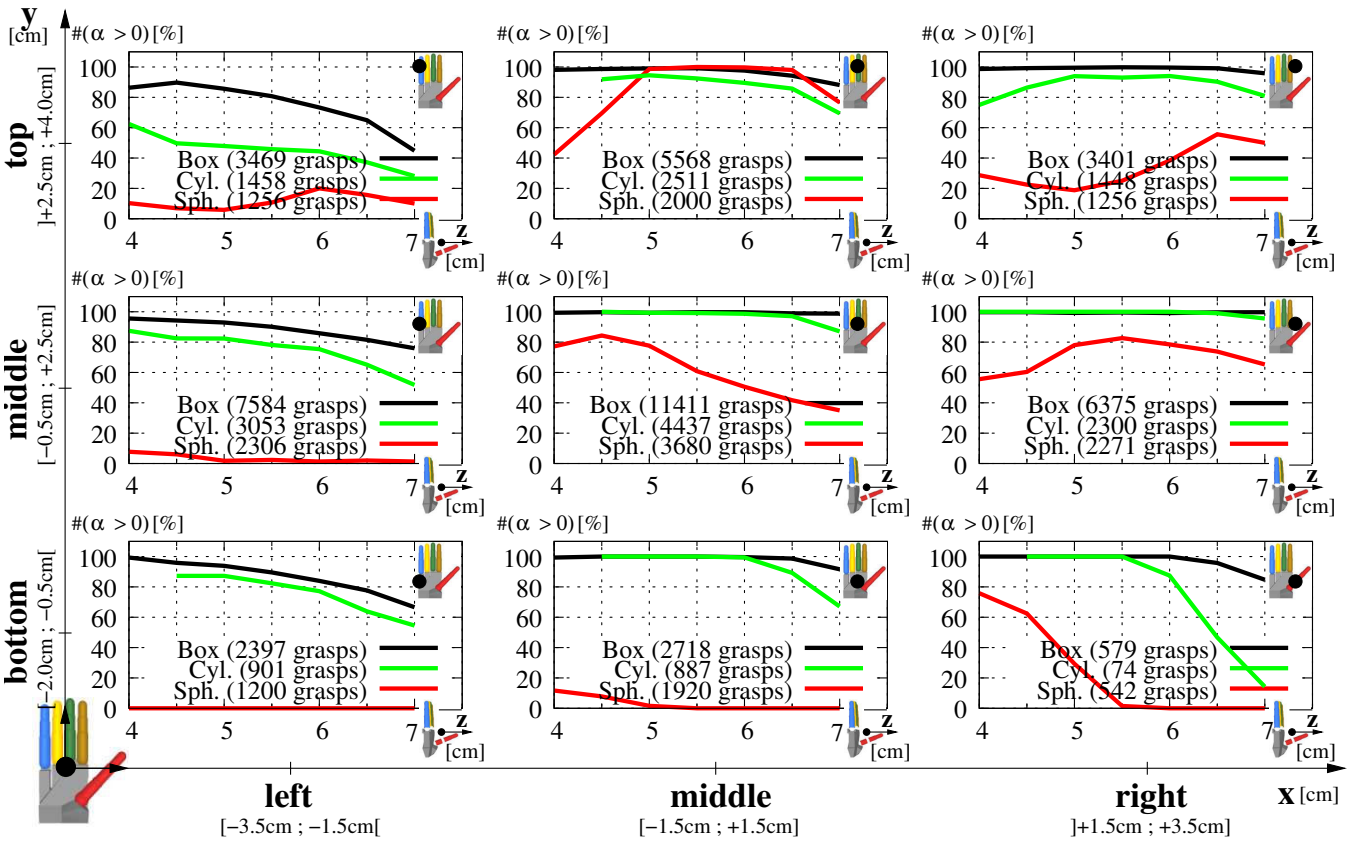

Fig. 4. Generalisation results for 77302 grasps (box: 43802, cylinder: 17069, sphere: 16431) in nine different object centre position regions in x-y-plane (parallel to palm; region cf. little figures in the upper right corners of each subgraph; position intervals: see overall-frame). Depicted are the percentages of accomplished force closure grasps ($\alpha > 0$) mapped onto the distance between palm and object centre (in z direction; z=4cm represents an object/hand distance near zero due to object and hand expansion). The number of grasps in each region is denoted in the according subgraph legend.

object, the evaluation of the grasp stability is conducted starting from various initial positions. These are selected from a regular grid spaced at 0.5 cm for cylinder and box, adding to a total of $15 \times 13 \times 7 = 1365$ positions, and spaced at 0.2 cm for the sphere resulting in $36 \times 31 \times 16 = 17.856$ positions. The grid dimensions can be read from the axis labels in Fig. 4 and are illustrated in Fig. 5. At each position the objects are also presented at $2 \times 4 \times 6 = 48$ different orientations (x: 0°, 45°; y: ±5°, ±15°; z: −45°– +5° spaced at 10°), where rotations about the x-axis are ignored for the cylinder and entirely for the sphere due to their symmetry.

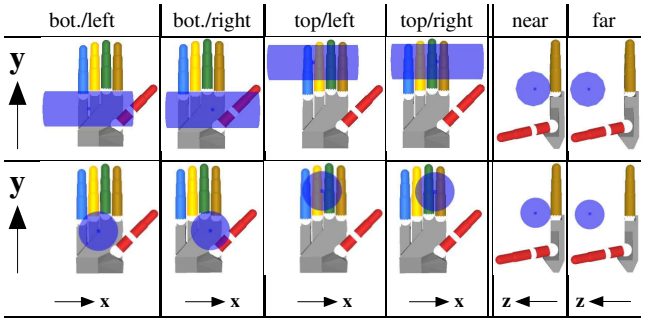

Fig. 5. Extremal initial positions of box/cylinder (first row) and sphere (second row) relative to the palm coordinate frame.

Initial configurations already causing collisions are ignored completely, which results in a total of 43.802 box grasps, 17.069 cylinder grasps and 16.431 sphere grasps.

To visualise the grasping results within this high-dimensional test space as concisely as possible, Fig. 4 displays the relative amount of force closure grasps (characterised by a grasp stability value $\alpha > 0$) averaged over all orientations and within nine subregions of the x-y-plane. The distance of the object centre to the palm (along z-axis) is shown most detailed within the sub figures, because it strongest affects the grasping result. Altogether, 79.53% of all grasps are force closure (box: 93.93%, cylinder: 83.41%, sphere: 37.12%), i.e. are stable with respect to any (small magnitude) disturbance wrench. Due to their similar object geometry, the evaluation outcome of the box and cylinder grasps are very similar in most object position regions whereas the number of force closure grasps for the cylinder stays almost always slightly below that for the box. Particular differences are on the one hand the lack of $z = 4$ values of the cylinder graphs in the middle and bottom positions caused by initial intersections at a distance $z = 4$ which are completely ignored for evaluation. On the other hand, a significantly faster decrease of the number of cylinder force closure grasps with increasing object/palm distance can be detected which is caused by a combination of a contact simulation stability

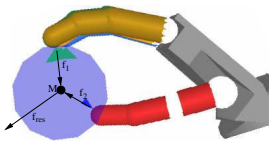

Fig. 6. If the fingers hardly reach round objects in distant positions, the net contact force f_{res} pushes the object away from the hand.

problem and the occurrence of a net object force pushing the object out of the grasp in the case of large object/hand distances (see Fig. 6). Additionally, the object can slide out of reach in the case of a misplaced first contact as the object movements are not constrained (e.g. by a table). The sphere can be grasped only in a very restricted position subspace. On the left side, the most crucial reason for the loss of performance is that the required hand postures can not be actuated appropriately (especially due to the restricted movability of the thumb) neither in the experience acquisition phase nor in the grasp execution itself. In the case of the right side regions, one drawback of the algorithm becomes apparent: as the algorithm cannot "see" the object before the first contact and it is not (yet) able to restart a grasp with another initial hand posture, the actuation of the situation-appropriate posture out of a disadvantageous posture can push the object apart and out of range. Similar to the box and the cylinder, the rate of force closure grasps decreases with increasing hand-object distance – again caused by a net contact force pushing the sphere away from the hand (Fig. 6).

Compared to an evaluation excluding the experience base, our new algorithm achieves a performance gain of +14.85% of all grasps (box: +18.11%, cyl.: +5.10%, sph.: +14.35%). The most distinct performance differences can be observed in the non-centre regions in which the experience-based algorithm proves to be more robust concerning the object position or the pregrasp respectively.

The same evaluation scheme using one *object-unspecific* 30x30 SOM (trained with all data of all objects) for all grasps results in less force closure grasps, outperforming the purely tactile-driven algorithm only in the case of the box. Altogether, the object-specific SOMs achieve +7.87% force closure grasps (box: +5.73%, cyl.: +4.98%, sph.: +16.60%).

V. Conclusion

We presented a new approach to dextrous robot grasping that dynamically combines grasping experience with current tactile object information. Searching for the grasp posture which best matches the current *Partial Contact Posture* the algorithm dynamically bridges the gap between general grasping knowledge and actual object perception. As an alternative experience representation, we introduced the *Grasp Manifold* being a smooth manifold in hand posture space. With the Self-Organising Map, we provided one powerful example of a *Grasp Manifold* approximation.

The presented approach using such *Grasp Manifolds* as experience base can provide force closure grasps for a great variety of grasp contexts. The generalisation ability has been shown in the evaluation where three SOMs with a total of 1875 nodes could generate force closure grasps in 79.53% of 77302 different object positions and orientations. As the algorithm does not plan the movement beforehand but dynamically adapts the grasping control according to the current grasp context, object displacements are handled without additional efforts. A certain robustness concerning the object shape is implicitly provided by the finalising generic finger closing heuristic which is independent of the experience base.

Future work will address an extension to more objects and more complex object shapes as well as a realisation of the presented grasp strategy with our real *ShadowHand* which does not meet the precision and tactile sensitivity requirements of the presented control algorithm yet. Furthermore, an incremental online training which is inherently supported by the SOM will be evaluated regarding to the benefits of developmental learning. Finally, the performance of continuous manifold representations like the *Unsupervised Kernel Regression* [5][6][7] will be evaluated concerning the effect of the continuity and the ability to represent whole movement trajectories instead of final grasp postures only.

References

[1] C. Borst, M. Fischer, and G. Hirzinger. Calculating hand configurations for precision and pinch grasps. In *Proc.IROS*, 2002.

[2] C. Borst, M. Fischer, and G. Hirzinger. Grasping the Dice by Dicing the Grasp. In *Proc. IROS*, 2003.

[3] CM-Labs. Vortex 2.1. www.cm-labs.com/products/vortex, 2005.

[4] R. Haschke, J. J. Steil, I. Steuwer, and H. Ritter. Task-oriented quality measures for dextrous grasping. In *Proc. Conference on Computational Intelligence in Robotics and Automation*. IEEE, 2005.

[5] S. Klanke and H. Ritter. A Leave-K-Out Cross-Validation Scheme for Unsupervised Kernel Regression. In *ICANN 2006*, volume 4132 of *LCNS*, pages 427–436. Springer, 2006.

[6] S. Klanke and H. Ritter. Variants of Unsupervised Kernel Regression: General Cost Functions. In *Proc. ESANN*, pages 581–586, Apr 2006.

[7] P. Meinicke, S. Klanke, R. Memisevic, and H. Ritter. Principal Surfaces from Unsupervised Kernel Regression. *IEEE Trans. on Pattern Analysis and Machine Intelligence*, 27(9):1379–1391, 2005.

[8] A. Miller and P. Allen. GraspIt!: A Versatile Simulator for Grasp Analysis. In *Proc. ASME Intl. Mechanical Engineering Congress & Exposition*, pages 1251–1258, 2000.

[9] A. Miller, S. Knoop, P. Allen, and H. Christensen. Automatic grasp planning using shape primitives. In *Proc. ICRA*, 2003.

[10] L. Natale and E. Torres-Jara. A sensitive approach to grasping. In *6th Intl. Conf. on Epigenetic Robotics, Paris, France*, 2006.

[11] R. Pelossof, A. Miller, P. Allen, and T. Jebara. An SVM Learning Approach to Robotic Grasping. In *Proc. ICRA*, 2004.

[12] R. Platt, A. Fagg, and R. Grupen. Nullspace Composition of Control Laws for Grasping. In *Proc. IROS*, 2002.

[13] R. Platt, A. Fagg, and R. Grupen. Manipulation Gaits: Sequences of Grasp Control Tasks. In *Proc. ICRA*, 2004.

[14] H. Ritter. Neo/NST The Graphical Simulation Toolkit. www.techfak.uni-bielefeld.de/ags/ni/projects/neo/neo_e.html.

[15] H. Ritter, T. Martinetz, and K. Schulten. *Neural Computation and Self-Organizing Maps*. Addison-Wesley, 1992.

[16] F. Röthling, R. Haschke, J. J. Steil, and H. Ritter. Platform Portable Anthropomorphic Grasping with the Bielefeld 20-DOF Shadow and 9-DOF TUM Hand, 2007. accepted for IROS 2007.

[17] J. Steffen. Erfahrungsbasierte Greifstrategie für anthropomorphe Roboterhände. Master's thesis, Bielefeld University, Dec 2005.

[18] J. Steil, F. Röthling, R. Haschke, and H. Ritter. Situated robot learning for multi-modal instruction and imitation of grasping. *Robotics and Autonomous Systems*, Special Issue on "Robot Learning by Demonstration"(47):129–141, 2004.

[19] The Shadow Robot Company. Shadow Dexterous Hand. www.shadowrobot.com/hand, 2002.